Desalination and Water Treatment
www.deswater.com
doi: 10.5004/dwt.2018.22769

123 (2018) 265–276
August

Studies of Cr(VI) adsorption on novel jute cellulose-kaolinite clay biocomposite

Md. Minhajul Islam[a], Shanta Biswas[a], M. Mehedi Hasan[b], Papia Haque[a], Sunzida H. Rimu[b], Mohammed Mizanur Rahman[a,b,*]

[a]*Department of Applied Chemistry and Chemical Engineering, Faculty of Engineering and Technology, University of Dhaka, Dhaka 1000, Bangladesh, Tel. +880-2-9661920-70/7392; Fax: +880-2-9667222; email: mizanur.rahman@du.ac.bd (M.M. Rahman)*
[b]*National Institute of Textile Engineering and Research, Nayarhat, Savar, Dhaka*

Received 13 February 2018; Accepted 5 July 2018

ABSTRACT

In this article, we have described the adsorption behavior of a biocomposite adsorbent prepared from crystalline cellulose of jute and kaolinite clay (locally available as Bijoypur clay). Despite lacking structural advantages such as smectite type montmorillonite clay used in other composites, this cellulose-clay composite showed good adsorption capacity. Cellulose was extracted from jute fiber and clay was modified with a surfactant named dodecylamine to prepare the biocomposite adsorbent. Effect of pH and contact time was investigated to figure out chromium adsorption capacity of the adsorbent. Maximum adsorption capacity was obtained at pH 4. The concentration of chromium in the test solution was determined by UV-spectrophotometer. The morphology of the composite was investigated using scanning electron microscope. Differential scanning calorimetry and thermogravimetric analysis of composite were carried out to investigate thermal behavior of the composite. The composite was characterized before and after adsorption experiment using Fourier-transform infrared spectroscopy and X-ray diffraction to validate the interaction of adsorbate chromium with adsorbent. Adsorption data of chromium by the adsorbent was analyzed according to Freundlich, Langmuir, Dubinin–Radushkevich, and Temkin adsorption models. Maximum adsorption capacity calculated from Langmuir isotherm model was 11.76 mg g^{-1} which was closer to results obtained experimentally. Pseudo-first-order, pseudo-second-order, and intraparticle diffusion kinetic models were proposed to understand the mechanism controlling the adsorption process. Moreover, this biocomposite was easily regenerated in sodium hydroxide solution and a maximum chromium desorption of 81.9% was achieved, which enabled the scope of reusability. Finally, a mechanism was proposed with illustration to show the adsorption potential of the composite.

Keywords: Biocomposite; Kaolinite; Crystalline cellulose; Chromium; Clay

1. Introduction

Last few decades have witnessed relentless expansion of urbanization and industrialization. This tremendous growth has brought about quite a few unwanted complications. Disturbance in ecosystem and threats to human health have been escalated by unadvised and improper release of hazardous materials to the environment as part of industrial wastes. Chromium, a heavy metal extensively used in compounds indispensable to tanning, metallurgy, textiles, and electroplating, etc., industry, has become a major concern for environmentalists due to its deleterious impact on human health. Chromium can exist in oxidation state ranging from 2+ to 6+, but in natural environment the most common oxidation states of chromium are chromium(III) and chromium(VI) [1]. While chromium(III) is less toxic and plays a significant role in glucose metabolism, chromium(VI) is starkly dangerous to aquatic life as well as human health and reportedly carcinogenic [2]. Moreover, the less harmful chromium(III) can be oxidized to chromium(VI) in the soil in presence of manganese oxides [3].

* Corresponding author.

So, it is of paramount importance to regulate the level of chromium released into nature by industries. To save the nature from further incorrigible damage, rigorous rules and regulations have been imposed regarding emission of hazardous materials such as chromium into nature [4]. The US Environmental Protection Agency has set a maximum contaminant limit of 0.1 mg L^{-1} for total chromium in drinking water [5]. While World Health Organization (WHO) has set stricter maximum permissible limit of total chromium in drinking water at 0.05 mg L^{-1} [6]. Therefore, the significance of chromium removal from industrial effluent is undeniable.

The precarious nature of hazardous metals and different organic toxification has led to development of wide range of treatment methods such as precipitation [7], coagulation-flocculation, sedimentation, flotation, filtration, membrane processes [8], electrochemical techniques [9], biological process [10], adsorption [11,12], and ion exchange methods with selectivity for specific types of ions [13,14]. Moreover, there have been some novel methods for combating organic pollutants. Sharma and Kumar et al. reported some works based on newly developed photodegradation [15–19] and photoozonation [20] methods. Among these techniques, adsorption has generated undeniable interest due to its economical approach, easy operation, and high efficiency. Adsorption can be defined as the selective transfer of solute onto the surface or into the bulk of a solid. Adsorption can proceed through different mechanisms such as intraparticle diffusion, external mass transfer, and adsorption at sites [21]. Adsorption equilibrium is a dynamic state where the adsorption of adsorbate molecules onto adsorbent surface is equal to the rate at which they desorb. While adsorption isotherm correlates the amount of adsorbate retained or released form liquid or gaseous phase to a solid phase. This correlation is graphically expressed with a curve by plotting amount adsorbed against concentration or pressure. The equilibrium isotherm is used to predict models of adsorption and adsorption system design. Moreover, various parameters and thermodynamic hypothesis can provide with a prediction about adsorption mechanism, surface phenomena, and degree of affinity of the adsorbent [22–26].

Cellulose, the most abundant natural polymer, is a polysaccharide containing hydroxyl groups in its structure, which act as a potent site for chromium adsorption. While clay is a readily available hydrous aluminosilicates containing exchangeable cations and anions on the surface, which work as active sites for heavy metal adsorption. A composite from these two biomaterials was fabricated to study chromium adsorption capacity by Santhana et al. [27], where the clay used was montmorillonite which is a 2:1 smectite type layered silicate [28]. We intended to investigate chromium adsorption capacity of crystalline cellulose-clay composite prepared from a structurally different type of clay. So, in our work a locally available kaolinite type clay, named Bijoypur white clay, is used to fabricate the composite. Unlike montmorillonite clay, kaolinite has 1:1 structure and there is no substitution of Si^{4+} with Al^{3+} in the tetrahedral layer and no substitution of Al^{3+} with other ions (e.g., Mg^{2+}, Zn^{2+}, Fe^{2+}, Ca^{2+}, Na^{+}, or K^{+}) in the octahedral layer. But as a result of presence of broken edges on the clay crystals, kaolinite has a small net negative charge. This negative charge, although small, is responsible for the surface not being completely inert [29].

In this study, a bioadsorbent was fabricated from crystalline cellulose and modified kaolinite clay to investigate chromium adsorption capacity. A thorough study of this composite's adsorption capacity has been investigated to figure out whether the structural difference has any significant bearing on its adsorption capacity. Furthermore, adsorption isotherms and kinetic models were developed and finally, a mechanism of adsorption process was proposed.

2. Materials and methods

2.1. Materials

Bijoypur clay was collected from Bijoypur area, Netrekona district by the help of Bangladesh Insulator and Sanitary Ware Factory (BISF), Mirpur, Dhaka, Bangladesh. Jute fiber was purchased from the local market of Bangladesh. All the chemicals used in this study were strictly analytical grade. Dodecylamine was brought from Sigma-Aldrich, 3050 Spruce Street, St. Louis, Sweden, hydrochloric acid from Merck KGaA, 64271 Damstadt, Germany, and sodium hydroxide was supplied by Loba Chemie Pvt. Ltd., 107, Mumbai 400005, India. Water was deionized for the purpose of using in composite preparation and adsorption study.

X-ray diffractometer (Bruker AXS Diffractometer D8, Germany) was used to carry out X-ray diffraction (XRD) analysis. An ATR-FTIR (Attenuated Total Reflectance/Fourier Transforms Infrared) spectrophotometer of model FT-IR8400S spectrophotometer, Shimadzu Corp, Japan was used. Spectroscopic grade dry KBr of 200 mg and 1 mg of powdered sample were ground in agate mortar. Pellets were formed from 100 mg of this ground mixture. Transmission band mode in the range 4,000–400 cm^{-1} was used to record the spectra with resolution being 4 cm^{-1} and hold time 5 min. Adsorption capacity was analyzed by a UV (Shimadzu 1700 UV) spectrophotometer. Scanning electron micrographs (SEM) images were taken at 20 kV with a JSM-6490LA, Jeol, Japan microscope. Differential scanning calorimetry (DSC) analysis was done using a DSC-60 (Shimadzu Corp, Japan) analyzer. The flow rate was maintained at 20 mL min^{-1}, temperature rate at 10 min^{-1}, and it was carried out in aluminum pan. In dry nitrogen environment heat change per gram of sample was recorded at a constant temperature for 60 min with a computerized system. Thermogravimetric analysis (TGA) was done using TG-00260 machine form Shimadzu Corp, Japan. To maintain inert atmosphere nitrogen gas supplied and the samples were taken in an aluminum cell. Temperature increase rate was maintained at 10°C min^{-1}, while hold time was 5 min. Initial and final temperatures were room temperature and 600°C, respectively.

2.2. Preparation of composite

Crystalline cellulose-clay composite was fabricated by the following methodology developed by Minhajul et al. [30]. Clay was modified with organophilic surfactant dodecyl amine [31] and crystalline cellulose crystal was extracted from jute fiber by hydrolysis using 40% sulfuric acid [32]. Modified clay was added to a 20 g LiOH-Urea-Water solution which was then agitated and frozen to a temperature of –12°C. Crystalline cellulose was added in this mixture and stirred for 10 min at 1,200 rpm until complete

dissolution. A proper blend of clay and crystalline cellulose crystal was obtained which was then allowed to rest and finally, acetone was added for crystalline cellulose regeneration. It was centrifuged again to separate crystalline cellulose-clay composite from liquid phase. The weight of clay and crystalline cellulose was varied to prepare composites of different weight ratios in such a way that composite MC1 had clay and crystalline cellulose ratio of 2:1, composite MC2 had clay and crystalline cellulose ratio of 1:1, and MC3 had similar 1:2 ratio.

2.3. Adsorption isotherm and kinetics study

Adsorption experiments were carried out in batch process at room temperature of 30°C ± 1°C. Chromium stock solution (1,000 ppm) was prepared by taking 0.2892 ± 0.0002 g potassium dichromate ($K_2Cr_2O_7$) in 100 mL volumetric flask. Stock solution was diluted to prepare desired 50 mg g^{-1} concentration of 25 mL chromium solution. 0.1 g composite was taken for adsorption study and solution pH 4 was adjusted by addition of 0.1 M NaOH and 0.1M H_2SO_4. The adsorption process was conducted using a reciprocating shaker for 300 min. After completion, the composite material was filtered from the solution and concentration of chromium before and after adsorption experiment was measured by a UV-spectrophotometer (Shimadzu 1700 UV) using 1,5-diphenyl carbazide procedure keeping wavelength fixed at 540 nm. This experiment was carried out three times in identical condition to ensure accuracy and reproducibility. Adsorption capacity q_e (mg g^{-1}) was calculated using the following equation:

$$q_e = \frac{(C_o - C_e) \times V}{W} \quad (1)$$

where C_o and C_e are initial and equilibrium concentration of chromium, respectively (mg L^{-1}). V is the volume of aqueous solution (L) and W is the weight of the adsorbent (g). The removal percentage R(%) which is defined as the ratio of differences in chromium concentration before and after adsorption experiment using Eq. (2) as follows:

$$R(\%) = \frac{C_i - C_e}{C_i} \times 100 \quad (2)$$

where C_i is the initial concentration of chromium in solution (mg L^{-1}) and C_e is the remaining concentration of chromium after adsorption (mg L^{-1}).

2.4. Regeneration of crystalline cellulose-clay composite

Desorption capability of adsorbents is a significant factor as it determines the reusability of adsorbents. Desorption of chromium from crystalline cellulose-clay adsorbent was carried out according to Tewari et al. [33]. A typical procedure for desorption of Cr(VI) from adsorbent MC1 composite was studied by using 0.1 N NaOH as eluent. Cr(VI) adsorbed composite was taken in 20 mL of 0.1 N NaOH into a 100 mL conical flask. After 90 min of shaking at 280°C and 120 rpm, the solution was centrifuged at 3,000 rpm for 10 min. The supernatant was analyzed for Cr(VI) concentration with the same procedure as done for adsorption study.

3. Results and discussion

3.1. Characterization of composite

FT-IR spectra of composite MC1 were measured before and after adsorption experiment and shown in Fig. S1. The figure showed that the composite exhibited characteristics peaks belonging to functional groups present in crystalline cellulose [34] and clay [35]. The peak assigned to –OH stretching stood out at 3,459 cm^{-1}. Several more peaks due to the stretching of –OH groups corresponding to the octahedral cations could be found at 3,696, 3,668, 3,653, and 3,619 cm^{-1}. Significant peaks from clay mineral were found at 1,114, 1,030, and 1,006 cm^{-1} due to Si–O stretching modes. Bending peaks of Al–Al–OH bonds were visible at 912 cm^{-1}. A strong band at 2,900 cm^{-1} was ascribed to C–H stretching present in dodecyl amine surfactant attached to clay due to modification. The band at 1,635 cm^{-1} could be due to H–OH bonding in water. In crystalline cellulose-clay composite, the quaternary ammonium cation attached to the modified clay created weak interaction with hydroxyl groups present in crystalline cellulose structure. Adsorption of chromium on the composite introduced deformation on the FT-IR spectra of –OH (3,651 cm^{-1}) region (Fig. S1(b)). As negatively charged bichromate ion was dominant in acidic solution of chromium [36], this ion interacted prominently with oppositely charged quaternary ammonium ion, resulting in palpable change in FT-IR spectra. In fact, this notion was strengthened by the presence of characteristic bond peak of Cr–O and Cr = O at 1,000–700 cm^{-1} regions [27].

XRD analysis of the composite, illustrated in Fig. 1, was carried out before and after Cr(VI) adsorption to investigate the crystalline nature of the biocomposite. Similar XRD analysis was carried out in other works to validate adsorption phenomena of the adsorbent [37–39]. Very distinct sharp peaks were observed which confirmed the crystalline nature of the composite. XRD patterns showed that different types of clay phases were present in the biocomposite. It

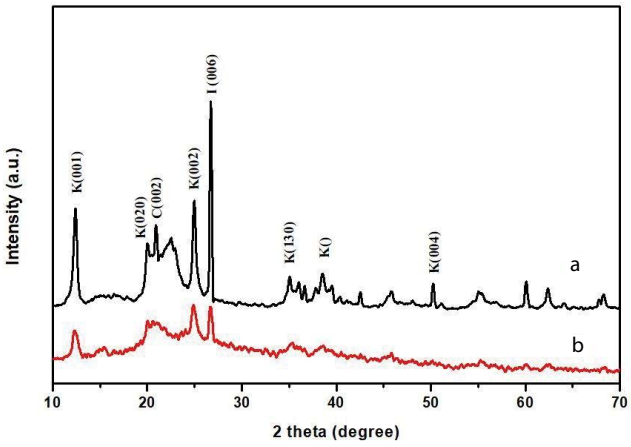

Fig. 1. XRD analysis of (a) MC1 composite before Cr(VI) adsorption, (b) MC1 composite after Cr(VI) adsorption (K = kaolinite, I = Illite, and C = crystalline cellulose).

was found that clay was predominated with kaolinite phase over other clay phases such as illite, chlorite, and quartz which concurred with the reported values in the literature. Peaks at 2θ = 12.47°, 19.55°, 24.96°, 35.05°, 36.07°, 38.43°, and 50.23° were corresponding to the (001), (020), (002), (130), (003), ($\bar{2}$02), and (004) planes, respectively, which were well defined crystalline peaks of kaolinite [40,41]. At 2θ = 22.55°, corresponding to (002) plane, peak of crystalline cellulose was observed [42]. Finally, peaks detected at 2θ = 20.90° were for (100) plane of quartz and 26.76° were for (006) diffraction plane of illite phase of the clay. Sharp and pointed diffraction peaks were found out in the patterns, which indicate the crystallinity of the composite and also the ordered nature of the layers of clays [43]. But after adsorption of chromium, the composite exhibited noticeable difference in the pattern (Fig. 1(b)). The distortion of peaks at 2θ region corresponding to 35°–40° implied changes due to adsorption of chromium on the adsorbent structure [44].

The surface morphology of composite MC1 was investigated by SEM. SEM of the prepared composite at different magnifications is shown in Fig. 2. The figure revealed that the surface (basal face) of the composite was irregular. There was variable roughness on the surface of the composite and broken edges on the contours. Two potential adsorption sites, broken bond surfaces at the edge and basal faces, were recognizable from the SEM images [45].

DSC and TGA thermograms are given in Figs. S2 and S3, respectively. DSC and TGA results revealed different thermal properties of the composites. Variation in weight ratio resulted in change in thermal behavior. Higher clay percentage in composite MC1 exhibited lower thermal degradation compared to composite with higher crystalline cellulose percentage MC3. This also indicated that the composite was able to withstand relatively high temperature (250°C) and maintain its structural integrity [30].

3.2. Effect of pH

The effect of pH holds a very important role in deciding the adsorption capacity of any adsorbent. The pH of solution influences the adsorption capacity by altering the surface properties of the adsorbent and ionic forms of chromium in solution. Optimization of pH for chromium adsorption by crystalline cellulose-clay adsorbent was carried out in pH range 2–10 while maintaining other parameters fixed (chromium solution concentration 50 mg L^{-1}, contact time 300 min, and adsorbent dose = 0.1 g). The pH range was adjusted by addition of 0.1 M NaOH and 0.1M H_2SO_4. The removal percentage was calculated using Eq. (2). From Fig. 3 it is clear that the effective removal of chromium was obtained between pH range 3.2–5.6 and maximum adsorption was found to be at pH 4, this is in accordance with other previous works of chromium adsorption by similar adsorbent [27,46].

This phenomenon could be attributed to metal ion interaction with functional groups present on the structure of adsorbent material. Chromium can exist as $HCrO_4^-$, CrO_4^{-2}, and $Cr_2O_7^{-2}$ depending on the pH and concentration of the solution [47]. But in lower pH range 3.8–5.5 chromium exists predominantly as bichromate ($HCrO_4^-$) ion. Moreover, at lower pH, the H^+ ions available in adsorption medium protonated amines groups available on the composite structure resulting in an electrostatic attraction between the positively charged functional groups on adsorbent and negatively charged metal ion adsorbate. While at higher pH, the deprotonation of hydroxyl groups created negatively charged sites on the composite structure and the negatively charged hydroxide ions in the solution started competing with similarly charged chromate ion (CrO_4^{2-}) which is predominant above pH 6. So, there was palpable reduction in removal percentage of chromium at higher pH [27].

3.3. Effect of contact time

Contact time of adsorbent and adsorbate is also an important parameter in determining equilibrium. The removal percentage increases gradually until the equilibrium point is reached. Experiments to figure out effect of contact time were carried out at fixed solution pH 4, 0.1 g of adsorbent and chromium solution of 50 mg g^{-1}. The removal percentage R(%) versus contact time are plotted in Fig. S4 and it is clear that there was a gradual increase in removal percentage of chromium until it reached 300 min. After that there was no significant change in removal percentage, which indicated that equilibrium point was reached. Crystalline cellulose-clay composite MC3 exhibited faster adsorption in initial stage due to higher content of crystalline cellulose in the composite. But maximum chromium removal percentage was observed for composite MC1 containing higher clay content. The faster initial adsorption rate of composite MC3 could be attributed to adsorption sites on crystalline cellulose, these sites were able to get into contact

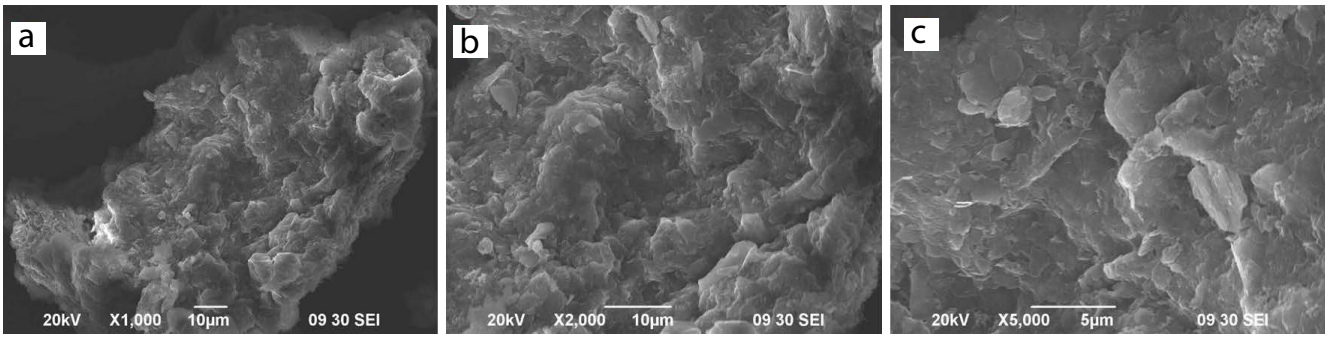

Fig. 2. SEM images of composite MC1 (a) at ×1,000, (b) at ×2,000, and (c) at ×5,000 magnification.

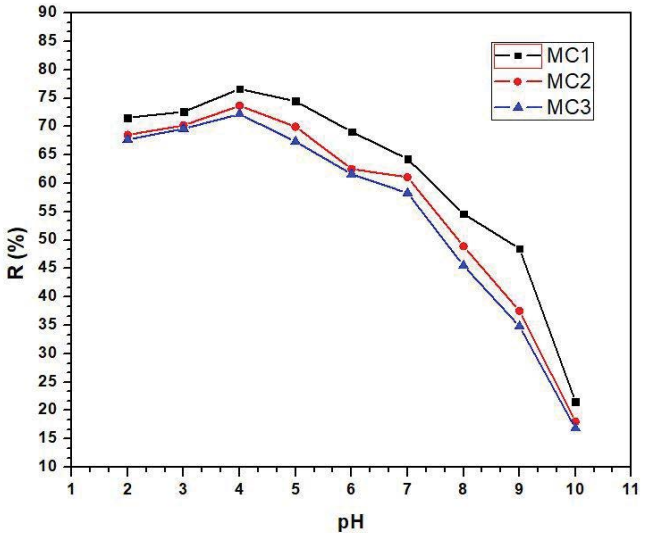

Fig. 3. Effect of pH on removal percentage R(%) of chromium by composites MC1, MC2, and MC3.

with adsorbate molecule faster than sites on clay structure. But eventual better adsorption by composite MC1 might be due to clay having multiple adsorption sites on the structure. The maximum experimental adsorption capacity was found to be 11.49 mg g^{-1} for composite MC1 at pH 4 and contact time 300 min.

3.4. Adsorption isotherms

In order to find out the sorption behavior of crystalline cellulose-clay composite, study of adsorption isotherms was carried out at room temperature. Composite used for adsorption isotherm study was MC1 which exhibited the highest removal percentage R(%). Langmuir isotherm correlates the equilibrium concentration of adsorbate and the amount adsorbed on the surface of the adsorbent. It is based on three assumptions that: (1) adsorption is monolayer in nature, (2) all adsorption sites are of equal size and shape, and (3) adsorbed molecules do not interact and adsorption is independent of adjacent sites [48]. The Langmuir isotherm model can be used to figure out maximum adsorption capacity by fitting experimental data to Langmuir isotherm model [49]. The Langmuir equation in linearized form is as follows:

$$\frac{C_e}{q_e} = \frac{1}{q_m b} + \frac{C_e}{q_m} \tag{3}$$

where C_e is the equilibrium concentration of chromium in mg L^{-1}, q_e is the amount of chromium adsorbed at equilibrium in mg g^{-1}, q_m is the maximum adsorption capacity in mg g^{-1}, and b is Langmuir constant (L mg^{-1}) related to energy of adsorption. The characteristics of Langmuir isotherm can be expressed by dimensionless separation factor, R_L, which is given by the following equation:

$$R_L = \frac{1}{1 + bC_o} \tag{4}$$

where C_o is the initial concentration of chromium in mg L^{-1} and b is the Langmuir constant (L mg^{-1}). R_L value indicates the chances of adsorption process being favorable when $0 < R_L < 1$, linear when $R_L > 1$, or irreversible when $R_L = 0$. The maximum adsorption capacity q_m and Langmuir constant b are obtained by plotting C_e/q_e against q_e from Eq. (3) and calculating the slope and intercept from it (Fig. 4). The Langmuir adsorption isotherm parameters are given in Table S1. For the current adsorbent, the R_L value is 0.10 which is between 0 and 1, thus establishing that adsorption of chromium on crystalline cellulose-clay composite is under favorable operating conditions [50,51]. A maximum homogeneous monolayer adsorption capacity (q_m) was calculated to be 11.76 mg g^{-1} from Langmuir isotherm model for composite MC1 which contains higher percentage of clay. This could be attributed to availability of double adsorption sites on clay surface. One is positively charged quaternary ammonium ion in surfactant due to modification and the other one being protonated $Si–OH^{2+}$.

Freundlich isotherm model is governed by heterogeneous multiplayer coverage. This model considers the logarithmic energy decrease with increasing surface coverage which arises from surface heterogeneity [52]. The linearized Freundlich equation is written as:

$$\log q_e = \log K_F + \frac{1}{n}\log C_e \tag{5}$$

where q_e is the amount of chromium adsorbed at equilibrium mg g^{-1}. C_e is the equilibrium concentration of chromium in solution in mg L^{-1}, K_F and n are Freundlich constants. K_F and n correspond to adsorption capacity and adsorption intensity, respectively. K_F and n values can be evaluated from the intercept and slope of logarithmic plot of q_e and C_e (Fig. 4) and were obtained as 1.475 and 1.41 where R^2 is 0.9997. The Freundlich adsorption isotherm parameters are given in Table S1.

The Freundlich constant n was found out to be between 1 and 10. This showed a favorable adsorption process and validity of classical Freundlich adsorption isotherm. Moreover, a larger value of n indicated that there had been effective interaction between adsorbent surface and chromium. Correlation coefficient R^2 implied that the experimental results fit the isotherm model.

The D–R isotherm, also known as Dubinin–Radushkevich isotherm, predicts the adsorption energy and the nature of adsorption mechanism. This isotherm is similar to Langmuir isotherm but D–R isotherm does not assume homogeneous surface or steady adsorption potential [53]. The linearized D–R isotherm Eq. (5) is as follows:

$$\ln q_e = \ln q_m - \beta\varepsilon^2 \tag{6}$$

where q_e is the amount of chromium(VI) adsorbed at equilibrium (mg g^{-1}), q_m is the maximum adsorption capacity (mg g^{-1}), β is a constant related to adsorption energy, and ε is Polanyi potential which is equal to:

$$\varepsilon = RT \times \ln\left(1 + \frac{1}{C_e}\right) \tag{7}$$

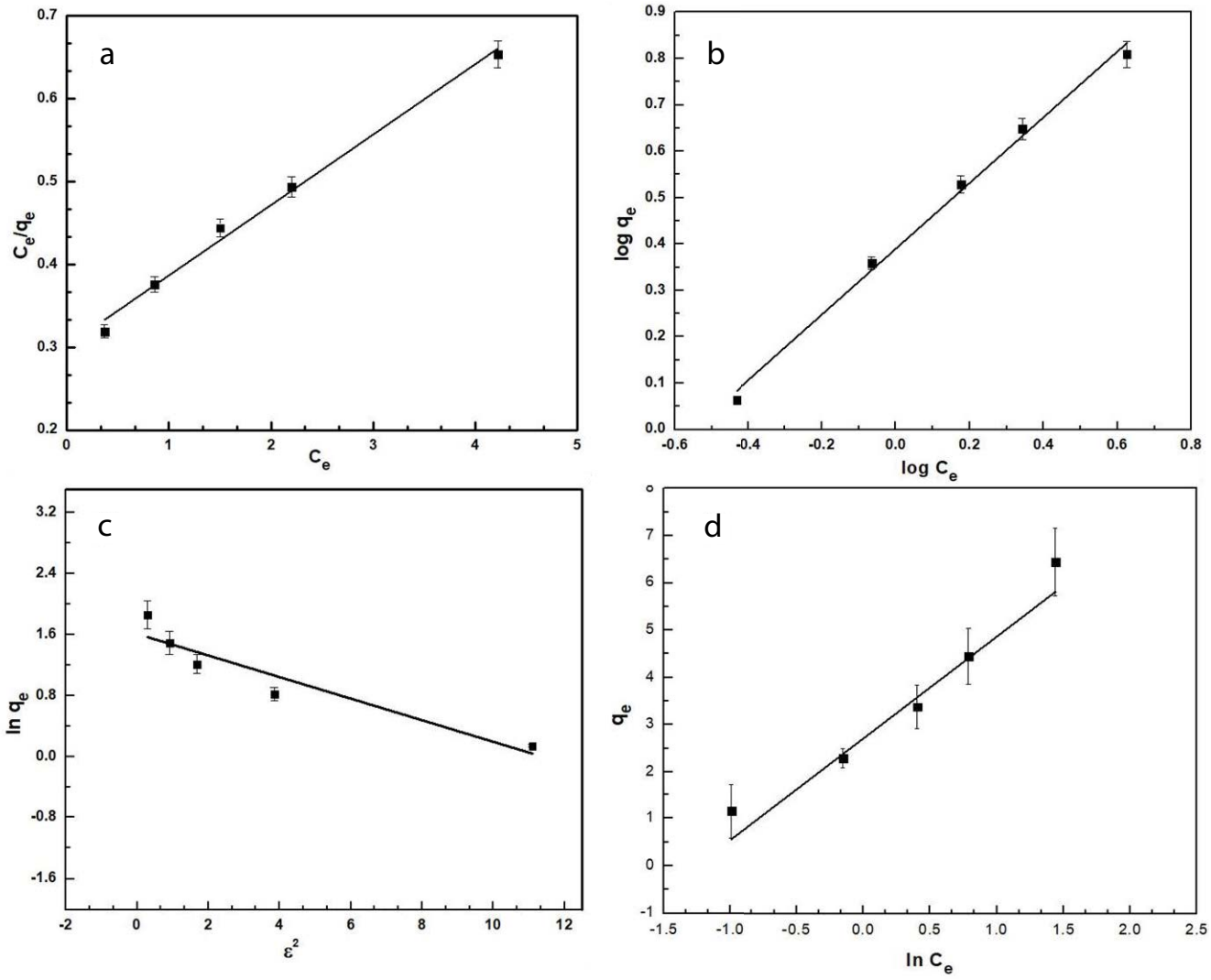

Fig. 4. (a) Langmuir adsorption isotherm, (b) Freundlich adsorption isotherm, (c) Dubinin–Radushkevich isotherm, and (d) Temkin isotherm for chromium adsorption by crystalline cellulose-clay composite.

where R is the gas constant 8.314 × 10^{-3} kJ mol^{-1} K^{-1} and T is the absolute temperature in K. Fig. 4 shows a plot of ln q_e versus ε^2. The values of β and q_m were evaluated from the slope and intercept of this plot (Fig. 4) and are presented in Table S1. The adsorption energy E was calculated using the relation $E = 1/\sqrt{(-2\beta)}$ where β = –0.141 mol^2kJ^{-2}, it was found to be +1.88. The positive value implied that this process was an endothermic adsorption having adsorption energy 1.88 kJ mol^{-1}. This indicated the electrostatic interaction between bichromate anion and adsorbent was endothermic and would be favored by higher temperature.

The assumption of Temkin isotherm model is that the heat of adsorption decreases linearly with surface coverage because of adsorbent and adsorbate interactions. The linear form of Temkin isotherm model is given by the following equation [54]:

$$q_e = \frac{RT}{b_T}\ln K_T + \frac{RT}{b_T}\ln C_e \quad (8)$$

where b_T is the Temkin constant related to the heat of adsorption (kJ mol^{-1}), T is the absolute temperature (K), K_T is the equilibrium binding constant corresponding to maximum binding energy (L g^{-1}), and R is the gas constant (8.314 × 10^{-3} kJ mol^{-1} K^{-1}).

Temkin constants were determined form the slope and intercept of ln C_e versus q_e curve (Fig. 4(d)). The parameters of Temkin isotherm are given in Table S1. The value of correlation coefficient showed that Temkin isotherm model fit with the experimental data. The bonding energy for ion-exchange mechanism is about 8–16 kJ mol^{-1} and the adsorption energy is less than −40 kJ mol^{-1} for physiosorption processes [55]. The value of b_T in this work implied that the adsorption process could be chemisorption.

3.5. Adsorption kinetics study

Different kinetics models were suggested to investigate the nature of adsorbents and mechanisms which govern the adsorption process. The goal was to find the best model

that supported the experimental data and figure out kinetic parameters of mass transfer of chromium from solution to adsorbent. So, the experimental data of chromium adsorption was tested using pseudo-first-order and pseudo-second-order kinetic models. The linearized forms of pseudo-first-order and pseudo-second-order kinetic models are shown in Eqs. (8) and (9) [56] as follows:

$$\text{Pseudo-first-order model, } \log\left(q_e - q_t\right) = \log q_e - \frac{k_1 t}{2.303} \quad (9)$$

$$\text{Pseudo-second-order model, } \frac{t}{q_t} = \frac{1}{h} + \frac{t}{q_e} \quad (10)$$

where q_t is the amount of chromium adsorbed on the surface at any time t, q_e is the amount of chromium adsorbed at equilibrium, h is the initial adsorption rate, and $h = k_2 q_e^2$. k_1 and k_2 are first-order and second-order rate constant, respectively.

The values of k_1 and q_e of pseudo-first-order reaction are obtained from the intercept and slope of the plot between log (q_e–q) versus t (Fig. 5(a)). While the values of k_2 and q_e are evaluated from the intercept and slope of plot between t/q_t versus t (Fig. 5(b)). The kinetic parameter data was tabulated and compared in Table 1.

The validity of the kinetic model was evaluated on the basis of correlation coefficient (R^2). The adsorption data is in accordance with pseudo-second-order model as the correlation coefficient is higher (>0.99) compared with other models. Maximum adsorption capacity q_e values obtained experimentally (11.49 mg g^{-1}) and calculated from the pseudo-second-order model (11.11 mg g^{-1}) are very close and this authenticated validity of pseudo-second-order model for this adsorption process. On the basis of assumption of pseudo-second-order model, it could be inferred that the rate-limiting step was the chemical sorption involving valence forces through sharing or exchange of electrons between adsorbent crystalline cellulose-clay composite and chromium [49].

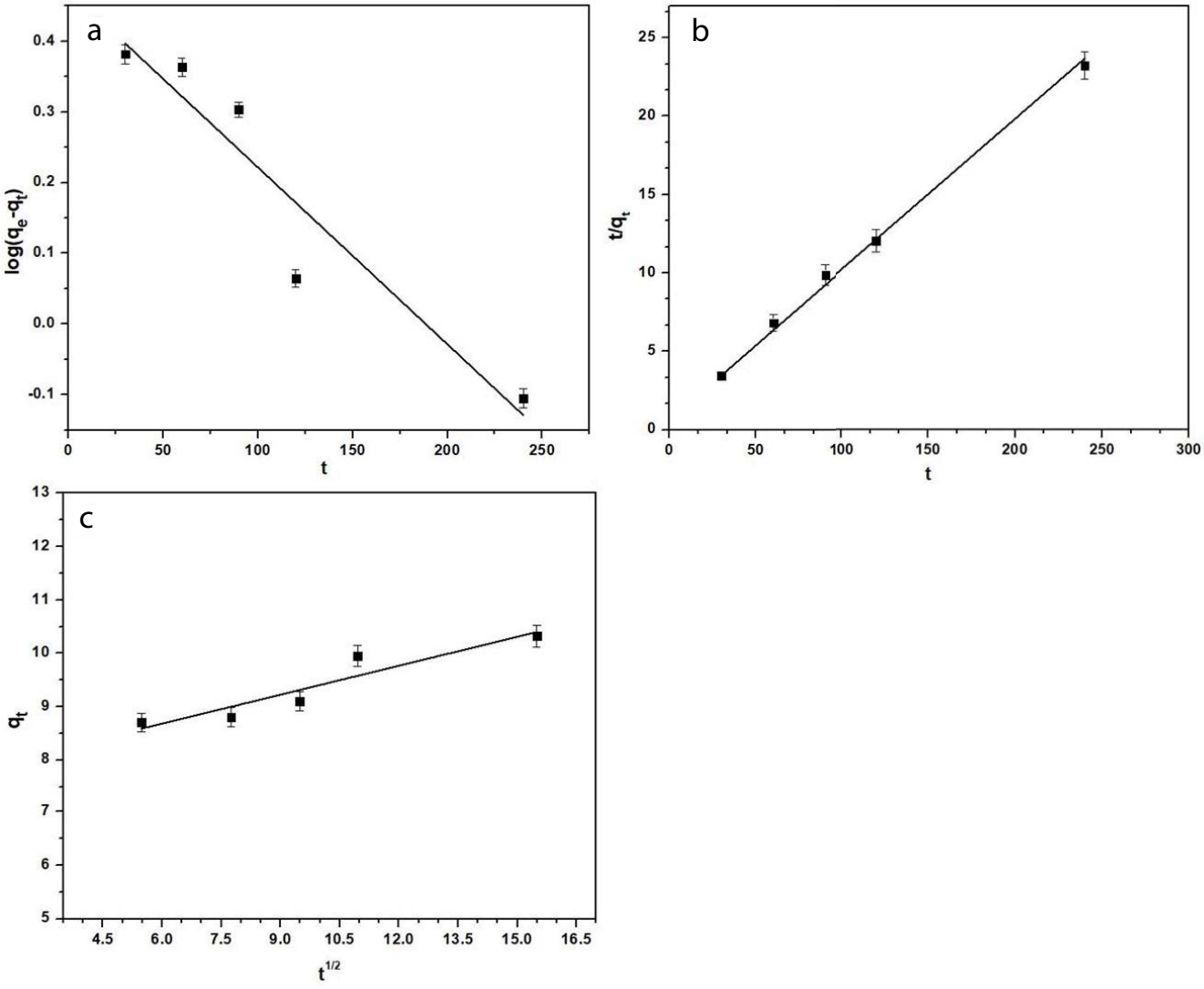

Fig. 5. (a) Pseudo-first-order, (b) pseudo-second-order, and (c) intraparticle diffusion plot for chromium adsorption by crystalline cellulose-clay composite.

Table 1
Kinetic parameters and intra particle rate constant for chromium adsorption

Model	Parameters	Composite (MC1)
Pseudo-first-order	k_1	0.005
	q_e	2.964
	R^2	0.87
Pseudo-second-order	K_2	0.014
	q_e	11.11
	R^2	0.99
Intraparticle diffusion	k_i	0.18

The Weber and Morris [57] intraparticle diffusion model parameters were calculated to determine whether film diffusion or intraparticle diffusion is the rate-limiting step. The model suggested that if the sorption mechanism is via intraparticle diffusion then a plot of q_t versus $t^{0.5}$ will be linear [27], and intraparticle diffusion is the sole rate-limiting step when such a plot passes through the origin. The Weber–Morris intraparticle diffusion model [57] is given by Eq. (11) as follows:

$$q_t = k_i t^{0.5} + C \tag{11}$$

where q_t is the amount of chromium adsorbed on the surface at any time t. k_i is the intraparticle rate constant (mg g^{-1} min$^{0.5}$). C (mg g^{-1}) is a constant related to the thickness of the boundary layer: the larger is the value of C, the greater is the boundary layer effect. The adsorption rate is influenced by the following steps: (1) film or surface diffusion, in which the adsorbate is transported from the bulk of the solution to the surface of adsorbent, (2) intraparticle or pore diffusion, in which the adsorbate species transfer into the interior part of the adsorbent, and (3) adsorption of adsorbate on the interior of adsorbent [58]. It is assumed that the adsorption process is not prominently influenced by adsorption kinetics as the adsorption process happens quite rapidly. The applicability of intraparticle diffusion as rate determining step is judged by Weber–Morris intraparticle diffusion model. From Fig. 5(c), it is evident that, the plot was almost linear and the presence of nonzero intercept implies that intraparticle diffusion was applicable but not the only controlling step in this adsorption process and the adsorption mechanism was governed by more than one mechanism [59].

3.6. Proposed mechanism of adsorption

The favorable adsorption of Cr(VI) was observed in weakly acidic medium. In lower pH, Cr(VI) exists in solution primarily as bichromate ($HCrO_4^-$) anion [47]. In case of crystalline cellulose, the only adsorption site is the –OH groups present on the hydrocarbon structure. The interaction between crystalline cellulose and bichromate ions is possible because of hydrogen bonding interaction between the hydroxyl groups of crystalline cellulose and bichromate anions [27].

On the other hand, two different sites for chromium adsorption are available in clay. One of them is the broken bond surfaces at the edge, while the other is the basal faces. These basal faces have charges which originate from isomorphous substitution within both tetrahedral and octahedral sheets [60,61]. The adsorption is due to mainly cation exchange and surface complexation. In this case, the surface at the amphoteric edges is the most relevant. This is because, at lower pH the hydroxyl group on the clay surface is converted to Si-OH^{2+}, resulting in interaction between bichromate ion ($HCrO_4^-$) and clay surface. Moreover, modification of clay with dodecyl amine has incorporated –NH_2 group into the structure. In acidic medium, this amine –NH_2 is converted into –NH_3^+. So, there is electrostatic attraction between positively charged –NH_3^+ and negatively charged bichromate ions. Another theory can be proposed based on Pearson's classification [62]. According to Pearson's classification, chromium is categorized as a hard acid and nitrogen is classified as a hard base. This can be used to explain the variety of complexation reactions. As they are both strong, good interaction between the positively charged protonated amine group of modified clay and negatively charged bichromate anion can be expected. Based on the experimental results and the information of the literature a proposed mechanism of chromium adsorption by crystalline cellulose-clay composite in weakly acidic medium (pH 4) is shown in Fig. 6.

3.7. Regeneration of crystalline cellulose-clay composite

Regeneration study plays a significant factor in determining the commercial potential of any adsorption procedure. In this experiment, a maximum chromium desorption of 81.9% was achieved, which indicated that the Cr(VI) loaded composite could be successfully regenerated. The result of the study showed that adsorption of Cr(VI) was not completely reversible but Cr(VI) ions could be desorbed from the surface of the composite. However, only ion exchange and physiosorption adsorbed Cr(VI) were desorbed [63]. The desorption process could be attributed to addition of NaOH which increased pH, consequently, decreasing H^+ ion in the solution. This in turn, brought about changes in functional groups attached to the adsorbent structure. Consequently, chromium adsorbed on the adsorbent surface due to electrostatic attraction and hydrogen bonding was released back to the solution.

3.8. Comparison with similar adsorbent

Many different types of adsorbents have been reported in literature for chromium adsorption [64,65]. The adsorption capacity of crystalline cellulose-clay composite was compared mainly with other similar polysaccharides, cellulose, or clay-based adsorbents reported in literature. The comparison is shown in Table 2 and it is evident from the table that crystalline cellulose-clay composite has competitive adsorption capacity for chromium. But crystalline cellulose-kaolinite clay composite exhibited lower adsorption capacity compared with crystalline cellulose–sodium montmorillonite composites [27]. This could be attributed to difference in clay structure. While sodium montmorillonite clay has intermolecular spacing and Na^+ plus other ion exchange sites,

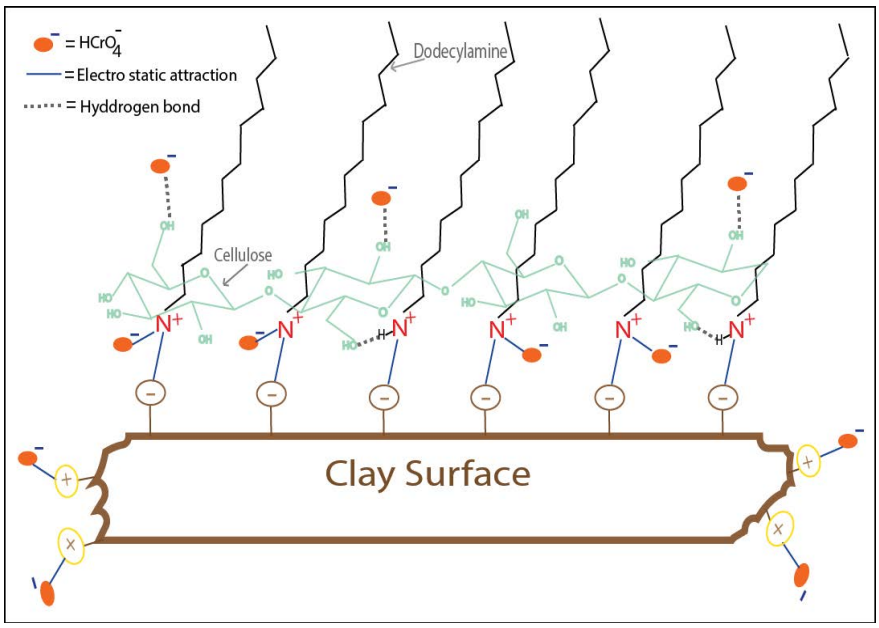

Fig. 6. Proposed mechanism of chromium adsorption by crystalline cellulose-clay composite in weakly acidic medium (pH 4).

Table 2
A comparison of adsorption capacity of similar adsorbents

No	Name of adsorbent	Adsorption capacity (mg g^{-1})	Reference
1.	Sugar bagasse (cellulosic adsorbent)	5.75	[66]
2.	Chitosan-sodium montmorillonite (unmodified clay) composite	9.36	[67]
3.	Maize corn (cellulosic adsorbent)	3.0	[66]
4.	Hexadecyltrimethylammonium bromide (HDTMA) modified montmorillonite clay	7.28	[68]
5.	Silica gel chitosan composite	3.5	[69]
6.	Activated carbon (from peanut shell activated with H_3PO_4)	46.73	[65]
7.	Activated carbon (from peanut shell activated with KOH)	13.89	[64]
8.	Crystalline cellulose-kaolinite clay composite	11.76	This work

kaolinite clay lacks interlayer cation exchange capabilities, thus resulting in lower adsorption of chromium. Two activated carbon adsorbents were included in the table to show that this adsorbent has adsorption capacity close to activated carbon obtained from peanut shell activated with KOH, but activated carbon activated with H_3PO_4 outperformed the adsorbent.

4. Conclusion

An adsorbent prepared from inexpensive and readily available materials crystalline cellulose and clay exhibited competitive chromium adsorption capacity in aqueous solution. Maximum adsorption capacity (11.76 mg g^{-1}) exhibited by the composite was better than what similar composites exhibited in other literature. Moreover, the experimental data successfully fitted Langmuir isotherm model and Freundlich isotherm model which indicated both homogenous and heterogeneous adsorption process were applicable for this adsorption process. The pseudo-second-order model described the kinetics of the adsorption process and established the notion that chemisorption was a possible adsorption mechanism. The experimental data fitted the Weber–Morris intraparticle diffusion model, which indicated the applicability of intraparticle diffusion for this adsorption process. The composite showed maximum chromium adsorption capacity at pH 4, which could be attributed to hydrogen bonding and electrostatic interaction between adsorbent and adsorbate. DSC and TGA thermal analysis showed good thermal stability of the composite. The adsorption was validated by FTIR and XRD analysis, where adsorption of chromium on the composite structure brought about significant alterations to the peaks. Not only effective removal capacity, but this composite was also able to exhibit impressive desorption capability. This offers scope for reusability of the composite and makes the adsorbent economically feasible for real-world utilization. Lastly, from this work we could conclude that adsorption capacity of composite prepared from kaolinite type clay was affected due to structural difference. Composite prepared from this type of clay exhibited lower adsorption capacity than the one made from smectite type of clay.

Acknowledgments

The author highly acknowledges to the Organization for the Prohibition of Chemical Weapons (OPCW) for their partial research grant (Project Account No: L/ICA/ICB/194479/14) to carry out the research.

References

[1] I. Tadesse, S.A. Isoaho, F.B. Green, J.A. Puhakka, Lime enhanced chromium removal in advanced integrated wastewater pond system, Bioresour. Technol., 97 (2006) 529–534.
[2] M. Owlad, M.K. Aroua, W.A.W. Daud, S. Baroutian, Removal of hexavalent chromium-contaminated water and wastewater: a review, Water Air Soil Pollut., 200 (2009) 59–77.
[3] R. Aravindhan, B. Madhan, J.R. Rao, B.U. Nair, T. Ramasami, Bioaccumulation of chromium from tannery wastewater: an approach for chrome recovery and reuse, Environ. Sci. Technol., 38 (2004) 300–306.
[4] K.Y. Foo, B.H. Hameed, Value-added utilization of oil palm ash: a superior recycling of the industrial agricultural waste, J. Hazard. Mater., 172 (2009) 523–531.
[5] H. Jabeen, V. Chandra, S. Jung, J.W. Lee, K.S. Kim, S.B. Kim, Enhanced Cr(vi) removal using iron nanoparticle decorated graphene, Nanoscale, 3 (2011) 3583–3585.
[6] WHO, Guidelines for Drinking-Water Quality, Geneva, 2011.
[7] M. Gheju, I. Balcu, Removal of chromium from Cr(VI) polluted wastewaters by reduction with scrap iron and subsequent precipitation of resulted cations, J. Hazard. Mater., 196 (2011) 131–138.
[8] P. Religa, A. Kowalik-Klimczak, P. Gierycz, Study on the behavior of nanofiltration membranes using for chromium(III) recovery from salt mixture solution, Desalination, 315 (2013) 115–123.
[9] P. Rana, N. Mohan, C. Rajagopal, Electrochemical removal of chromium from wastewater by using carbon aerogel electrodes, Water Res., 38 (2004) 2811–2820.
[10] Y. Chen, G. Gu, Preliminary studies on continuous chromium(VI) biological removal from wastewater by anaerobic–aerobic activated sludge process, Bioresour. Technol., 96 (2005) 1713–1721.
[11] H. Leinonen, J. Lehto, Purification of metal finishing waste waters with zeolites and activated carbons, Waste Manage. Res., 19 (2001) 45–57.
[12] G. Sharma, M. Naushad, A. Kumar, S. Rana, S. Sharma, A. Bhatnagar, F.J. Stadler, A.A. Ghfar, M.R. Khan, Efficient removal of coomassie brilliant blue R-250 dye using starch/poly(alginic acid-cl-acrylamide) nanohydrogel, Process Saf. Environ. Protect., 109 (2017) 301–310.
[13] S. Mustafa, K.H. Shah, A. Naeem, M. Waseem, M. Tahir, Chromium (III) removal by weak acid exchanger Amberlite IRC-50 (Na), J. Hazard. Mater., 160 (2008) 1–5.
[14] G. Sharma, B. Thakur, M. Naushad, A.A.H. Al-Muhtaseb, A. Kumar, M. Sillanpaa, G.T. Mola, Fabrication and characterization of sodium dodecyl sulphate@ironsilicophosphate nanocomposite: ion exchange properties and selectivity for binary metal ions, Mater. Chem. Phys., 193 (2017) 129–139.
[15] D. Pathania, G. Sharma, A. Kumar, M. Naushad, S. Kalia, A. Sharma, Z.A. Alothman, Combined sorptional–photocatalytic remediation of dyes by polyaniline Zr(IV) selenotungstophosphate nanocomposite, Toxicol. Environ. Chem., 97 (2015) 526–537.
[16] D. Pathania, D. Gupta, A.A.H. Al-Muhtaseb, G. Sharma, A. Kumar, M. Naushad, T. Ahamad, S.M. Alshehri, Photocatalytic degradation of highly toxic dyes using chitosan-g-poly(acrylamide)/ZnS in presence of solar irradiation, J. Photochem. Photobiol. A: Chem., 329 (2016) 61–68.
[17] A. Kumar, Shalini, G. Sharma, M. Naushad, A. Kumar, S. Kalia, C. Guo, G.T. Mola, Facile hetero-assembly of superparamagnetic Fe3O4/BiVO4 stacked on biochar for solar photo-degradation of methyl paraben and pesticide removal from soil, J. Photochem. Photobiol. A: Chem., 337 (2017) 118–131.
[18] G. Sharma, M. Naushad, A. Kumar, S. Devi, M.R. Khan, Lanthanum/cadmium/polyaniline bimetallic nanocomposite for the photodegradation of organic pollutant, Iran. Polym. J., 24 (2015) 1003–1013.
[19] A. Kumar, A. Kumar, G. Sharma, A.A.H. Al-Muhtaseb, M. Naushad, A.A. Ghfar, F.J. Stadler, Quaternary magnetic BiOCl/g-C3N4/Cu2O/Fe3O4 nano-junction for visible light and solar powered degradation of sulfamethoxazole from aqueous environment, Chem. Eng. J., 334 (2018) 462–478.
[20] A. Kumar, A. Kumar, G. Sharma, M. Naushad, F.J. Stadler, A.A. Ghfar, P. Dhiman, R.V. Saini, Sustainable nano-hybrids of magnetic biochar supported g-C3N4/FeVO4 for solar powered degradation of noxious pollutants- Synergism of adsorption, photocatalysis and photo-ozonation, J. Cleaner Prod., 165 (2017) 431–451.
[21] X.-S. Wang, Y. Qin, Equilibrium sorption isotherms for of Cu2+ on rice bran, Process Biochem., 40 (2005) 677–680.
[22] G. Limousin, J.P. Gaudet, L. Charlet, S. Szenknect, V. Barthès, M. Krimissa, Sorption isotherms: a review on physical bases, modeling and measurement, Appl. Geochem., 22 (2007) 249–275.
[23] S.J. Allen, G. McKay, J.F. Porter, Adsorption isotherm models for basic dye adsorption by peat in single and binary component systems, J. Colloid Interf. Sci., 280 (2004) 322–333.
[24] K. Vasanth Kumar, S. Sivanesan, Sorption isotherm for safranin onto rice husk: comparison of linear and non-linear methods, Dyes Pigm., 72 (2007) 130–133.
[25] M. Ghiaci, A. Abbaspur, R. Kia, F. Seyedeyn-Azad, Equilibrium isotherm studies for the sorption of benzene, toluene, and phenol onto organo-zeolites and as-synthesized MCM-41, Sep. Purif. Technol., 40 (2004) 217–229.
[26] M.C. Ncibi, Applicability of some statistical tools to predict optimum adsorption isotherm after linear and non-linear regression analysis, J. Hazard. Mater., 153 (2008) 207–212.
[27] A.S.K. Kumar, S. Kalidhasan, V. Rajesh, N. Rajesh, Application of cellulose-clay composite biosorbent toward the effective adsorption and removal of chromium from industrial wastewater, Ind. Eng. Chem. Res., 51 (2012) 58–69.
[28] M. Darder, E. Ruiz-Hitzky, Caramel-clay nanocomposites, J. Mater. Chem., 15 (2005) 3913–3918.
[29] K.G. Bhattacharyya, S.S. Gupta, Adsorption of a few heavy metals on natural and modified kaolinite and montmorillonite: a review, Adv. Colloid Interface Sci., 140 (2008) 114–131.
[30] M.M. Islam, M. Nuruzzaman Khan, S. Biswas, T.R. Choudhury, P. Haque, T.U. Rashid, M.M. Rahman, Preparation and characterization of bijoypur clay-crystalline cellulose composite for application as an adsorbent, Adv. Mater. Sci., 2 (2017) 1–7.
[31] A.N. Nakagaito, H. Yano, The effect of fiber content on the mechanical and thermal expansion properties of biocomposites based on microfibrillated cellulose, Cellulose, 15 (2008) 555–559.
[32] M.M. Rahman, S. Afrin, P. Haque, M.M. Islam, M.S. Islam, M.A. Gafur, Preparation and characterization of jute cellulose crystals-reinforced poly(L-lactic acid) biocomposite for biomedical applications, Int. J. Chem. Eng., 2014 (2014) 7.
[33] N. Tewari, B. Guha, P. Vasudevan, Adsorption study of hexavalent chromium by bentonite clay, Asian J. Chem., 17 (2005) 2184.
[34] C.-F. Liu, R.-C. Sun, A.-P. Zhang, M.-H. Qin, J.-L. Ren, X.-A. Wang, Preparation and characterization of phthalated cellulose derivatives in room-temperature ionic liquid without catalysts, J. Agric. Food Chem., 55 (2007) 2399–2406.
[35] M.A. Hossain, Y. Zaker, M. Ali, M.S. Islam, T.S.A. Islam, Characterization of sand fractionated from Bijoypur soil, Bangladesh and its application as an adsorbent, Res. J. Chem. Sci., 3 (2013) 90–94.
[36] P. Suksabye, P. Thiravetyan, W. Nakbanpote, S. Chayabutra, Chromium removal from electroplating wastewater by coir pith, J. Hazard. Mater., 141 (2007) 637–644.
[37] A.A. Alqadami, M. Naushad, M.A. Abdalla, M.R. Khan, Z.A. Alothman, Adsorptive removal of toxic dye using Fe3O4–TSC nanocomposite: equilibrium, kinetic, and thermodynamic studies, J. Chem. Eng. Data, 61 (2016) 3806–3813.

[38] M. Naushad, T. Ahamad, B.M. Al-Maswari, A. Abdullah Alqadami, S.M. Alshehri, Nickel ferrite bearing nitrogen-doped mesoporous carbon as efficient adsorbent for the removal of highly toxic metal ion from aqueous medium, Chem. Eng. J., 330 (2017) 1351–1360.
[39] A.A. Alqadami, M. Naushad, Z.A. Alothman, A.A. Ghfar, Novel metal–organic framework (MOF) based composite material for the sequestration of U(VI) and Th(IV) metal ions from aqueous environment, ACS Appl. Mater. Interface, 9 (2017) 36026–36037.
[40] M.S. Miran, M.Y.A. Mollah, A. Hussain, M.M. Rahman, A multi-technique characterization of Bijoypur clay, Bangladesh J. Sci. Res., 21 (2008) 15–22.
[41] D.P. Ajanta Sachan, Identification of microfabric of kaolinite clay mineral using X-ray diffraction technique. Geotech. Geol. Eng., 25 (2007) 603.
[42] C. Xu, S. Zhu, C. Xing, D. Li, N. Zhu, H. Zhou, Isolation and properties of cellulose nanofibrils from coconut palm petioles by different mechanical process, PLoS One, 10 (2015) e0122123.
[43] A.K. Ghosh, E.M. Woo, Effects of layered silicates on the confined crystalline morphology of poly(hexamethylene terephthalate), J. Mater. Chem., 14 (2004) 3034–3042.
[44] C.-K. Lin, J.-N. Chen, C.-C. Lin, An NMR, XRD and EDS study of solidification/stabilization of chromium with Portland cement and C3S, J. Hazard. Mater., 56 (1997) 21–34.
[45] M.B. Hocking, K.A. Klimchuk, S. Lowen, Polymeric flocculants and flocculation, J. Macromol. Sci., Part C, 39 (1999) 177–203.
[46] R. Karthik, S. Meenakshi, Removal of hexavalent chromium ions using polyaniline/silica gel composite, J. Water Process Eng., 1 (2014) 37–45.
[47] P. Luo, J.-S. Zhang, B. Zhang, J.-H. Wang, Y.-F. Zhao, J.-D. Liu, Preparation and characterization of silane coupling agent modified halloysite for Cr(VI) removal, Ind. Eng. Chem. Res., 50 (2011) 10246–10252.
[48] P.P. Atkins, J. de Paula, Elements of Physical Chemistry, Oxford University Press, New Delhi, India, 2009.
[49] I. Langmuir, The adsorption of gases on plane surfaces of glass, mica and platinum, J. Am. Chem. Soc., 40 (1918) 1361–1403.
[50] J. Febrianto, A.N. Kosasih, J. Sunarso, Y.-H. Ju, N. Indraswati, S. Ismadji, Equilibrium and kinetic studies in adsorption of heavy metals using biosorbent: a summary of recent studies, J. Hazard. Mater., 162 (2009) 616–645.
[51] P. Beneš, V. Majer, Trace Chemistry of Aqueous Solutions: General Chemistry and Radiochemistry, Elsevier, New York, 1980.
[52] H. Freundlich, Over the adsorption in solution, J. Phys. Chem., 57 (1906) 1100–1107.
[53] S. Chatterjee, D.S. Lee, M.W. Lee, S.H. Woo, Nitrate removal from aqueous solutions by cross-linked chitosan beads conditioned with sodium bisulfate, J. Hazard. Mater., 166 (2009) 508–513.
[54] B. Kiran, A. Kaushik, Chromium binding capacity of *Lyngbya putealis* exopolysaccharides, Biochem. Eng. J., 38 (2008) 47–54.
[55] H.F. Walton, Ion exchange, J. Chem. Educ., 23 (1946) 454.
[56] J. He, R. Lin, H. Long, Y. Liang, Y. Chen, Adsorption characteristics of amino acids on to calcium oxalate, J. Colloid Interface Sci., 454 (2015) 144–151.
[57] W.J.M. Weber, J.C. Morris, Kinetics of adsorption on carbon from solution, J. Sanit. Eng. Div., 89 (1963) 31–60.
[58] H.K. Boparai, M. Joseph, D.M. O'Carroll, Kinetics and thermodynamics of cadmium ion removal by adsorption onto nano zerovalent iron particles, J. Hazard. Mater., 186 (2011) 458–465.
[59] S.A. Drweesh, N.A. Fathy, M.A. Wahba, A.A. Hanna, A.I. Akarish, E.A. Elzahany, I.Y. El-Sherif, K.S. Abou-El-Sherbini, Equilibrium, kinetic and thermodynamic studies of Pb (II) adsorption from aqueous solutions on HCl-treated Egyptian kaolin, J. Environ. Chem. Eng., 4 (2016) 1674–1684.
[60] B. Baeyens, M.H. Bradbury, A mechanistic description of Ni and Zn sorption on Na-montmorillonite Part I: titration and sorption measurements, J. Contam. Hydrol., 27 (1997) 199–222.
[61] F.J. Huertas, L. Chou, R. Wollast, Mechanism of kaolinite dissolution at room temperature and pressure Part II: kinetic study, Geochim. Cosmochim. Acta, 63 (1999) 3261–3275.
[62] R.G. Pearson, Hard and soft acids and bases, J. Am. Chem. Soc., 85 (1963) 3533–3539.
[63] L. Deng, Z. Shi, L. Luo, S.-Y. Chen, L.-F. Yang, X.-Z. Yang, L.-S. Liu, Adsorption of hexavalent chromium onto kaolin clay based adsorbent, J. Central South Univ., 21 (2014) 3918–3926.
[64] Z.A. Al-Othman, R. Ali, M. Naushad, Hexavalent chromium removal from aqueous medium by activated carbon prepared from peanut shell: adsorption kinetics, equilibrium and thermodynamic studies, Chem. Eng. J., 184 (2012) 238–247.
[65] Z.A. Alothman, M. Naushad, R. Ali, Kinetic, equilibrium isotherm and thermodynamic studies of Cr(VI) adsorption onto low-cost adsorbent developed from peanut shell activated with phosphoric acid, Environ. Sci. Pollut. Res., 20 (2013) 3351–3365.
[66] U.K. Garg, M.P. Kaur, V.K. Garg, D. Sud, Removal of hexavalent chromium from aqueous solution by agricultural waste biomass, J. Hazard. Mater., 140 (2007) 60–68.
[67] J.-H. An, S. Dultz, Adsorption of Cr (VI) and As (V) on chitosan-montmorillonite: selectivity and pH dependence, Clays Clay Miner., 56 (2008) 549–557.
[68] S.T. Akar, Y. Yetimoglu, T. Gedikbey, Removal of chromium (VI) ions from aqueous solutions by using Turkish montmorillonite clay: effect of activation and modification, Desalination, 244 (2009) 97–108.
[69] M.R. Gandhi, S. Meenakshi, Preparation and characterization of La (III) encapsulated silica gel/chitosan composite and its metal uptake studies, J. Hazard. Mater., 203 (2012) 29–37.

Supplementary Information

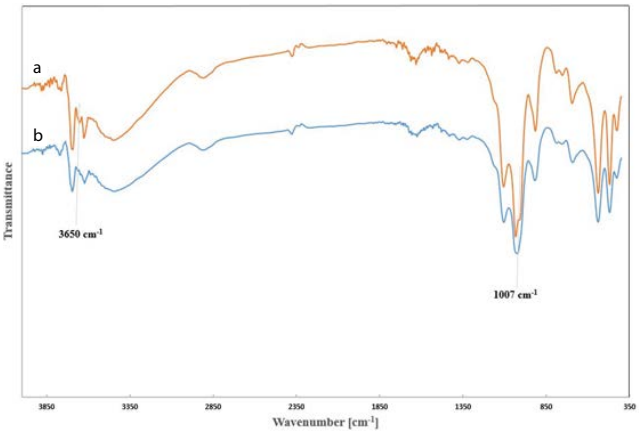

Fig. S1. FTIR analysis of (a) composite MC1 before adsorption, (b) after adsorption of chromium.

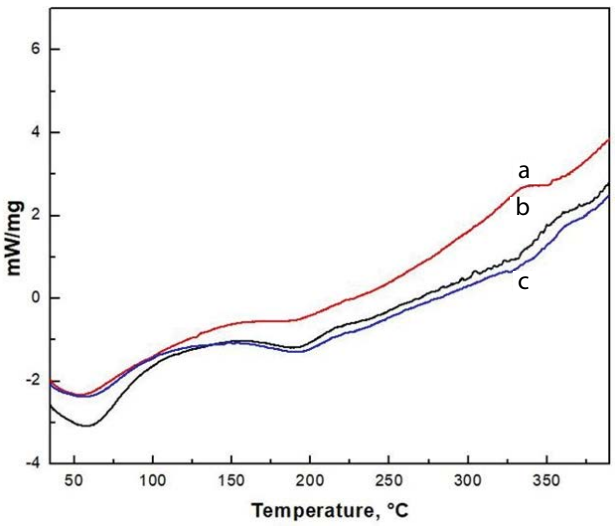

Fig. S2. DSC analysis of composite (a) MC1, (b) MC2, and (c) MC3.

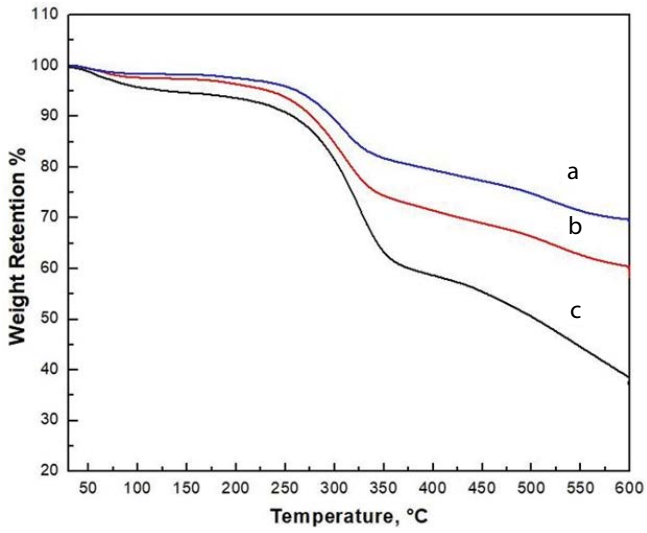

Fig. S3. TGA analysis of composite (a) MC1, (b) MC2, and (c) MC3.

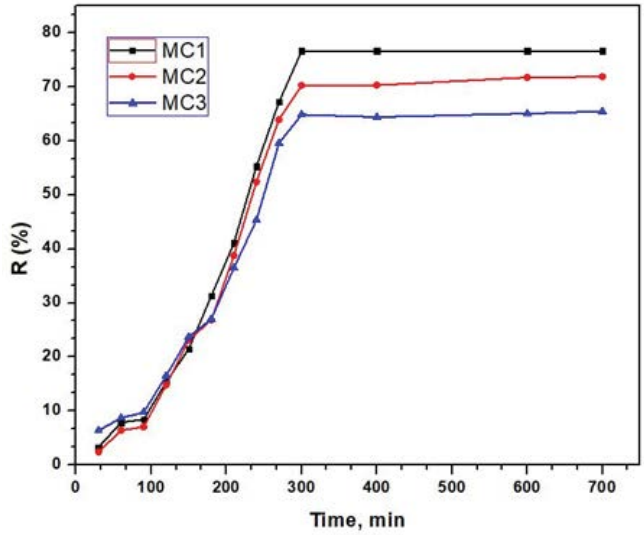

Fig. S4. Effect of contact time on chromium adsorption by crystalline cellulose-clay composite.

Table S1
Different parameters of Langmuir, Freundlich, Dubinin–Radushkevich, and Temkin isotherms.

Langmuir isotherm	q_m (mg g^{-1})	b (L mg^{-1})	R_L	R^2
	11.76	0.282	0.105	0.99
Freundlich isotherm	K_F	n	R^2	
	1.475	1.41	0.99	
Dubinin–Radushkevich isotherm	β (mol^2 kJ^{-2})	E (kJ mol^{-1})	R^2	
	1.475	1.88	0.86	
Temkin isotherm	b_T (kJ mol^{-1})	k_T (L g^{-1})	R^2	
	1.154	3.479	0.94	